Letter

Engineering long-range molecular potentials by external drive

Tanita Klas,[1] Jana Bender,[1] Patrick Mischke,[1,2] Thomas Niederprüm,[1] and Herwig Ott[1,*]

[1]*Department of Physics and Research Center OPTIMAS, Rheinland-Pfälzische Technische Universität Kaiserslautern-Landau, 67663 Kaiserslautern, Germany*

[2]*Max Planck Graduate Center with the Johannes Gutenberg-Universität Mainz (MPGC), Staudinger Weg 9, 55128 Mainz, Germany*

(Received 14 March 2023; accepted 7 July 2023; published 21 August 2023)

We report the engineering of molecular potentials at large interatomic distances. The molecular states are generated by off-resonant optical coupling to a highly excited, long-range Rydberg molecular potential. The coupling produces a potential well in the low-lying molecular potential, which supports a bound state. The depth of the potential well, and thus the binding energy of the molecule, can be tuned by the coupling parameters. We characterize these molecules and find good agreement with a theoretical model based on the coupling of the two involved adiabatic potential energy curves. Our results open numerous possibilities to create long-range molecules between ultracold ground-state atoms and to use them for ultracold chemistry and applications such as Feshbach resonances, Efimov physics, or the study of halo molecules.

DOI: 10.1103/PhysRevA.108.L021301

The interaction between individual atoms is determined by the interparticle molecular potentials. They are responsible for the scattering properties and the appearance of bound molecular states. Consequently, a substantial effort is put into properly understanding and controlling interaction potentials, especially in the context of ultracold atomic gases. A controlled deformation or tailoring of molecular potentials bears great potential for ultracold chemistry applications and few-body physics but is an ambitious task since the molecular potentials are fixed by the atomic properties.

Attempts towards the potential engineering of low-lying states for scattering processes have attracted considerable attention in the context of magnetic [1] and optical [2] Feshbach resonances. These have sparked a wide range of advances in many-body physics as the association of ultracold molecules [3,4], the formation of molecular Bose-Einstein condensates [5,6], and ultracold dipolar molecular systems [7]. Macrodimer Rydberg dressing has been demonstrated to create a distance-selective interaction in an optical lattice between two ground-state atoms at a micrometer distance [8]. However, engineering low-lying molecular potentials in such a way that new bound molecular states emerge has remained elusive so far. The control on the molecules' vibrational and rotational state turns potential engineering into a promising platform for ultracold chemistry [9].

Here, we demonstrate a generic scheme on how to use strong optical coupling to transfer the desired characteristics of an auxiliary potential to a target potential. In particular, we couple an auxiliary potential with a potential well at a large interatomic separation to a short-range target potential as shown in Fig. 1. If, at the interatomic distance of interest, the modulation of the auxiliary potential is large compared to that of the target potential, the character of the auxiliary potential is admixed to the target potential. The resulting molecular potential inherits the short-range physics from the target state but features an additional potential well at much larger internuclear distances. If the coupling is strong enough, a bound molecular state emerges. The designed molecules do not compete in their characteristics with the conventional, short-range $5S$-$6P$ molecules. While for the present experimental parameters binding energies of up to $-h \times 40\,\mathrm{MHz}$ and bond lengths of $950a_0$ are expected, the highest lying

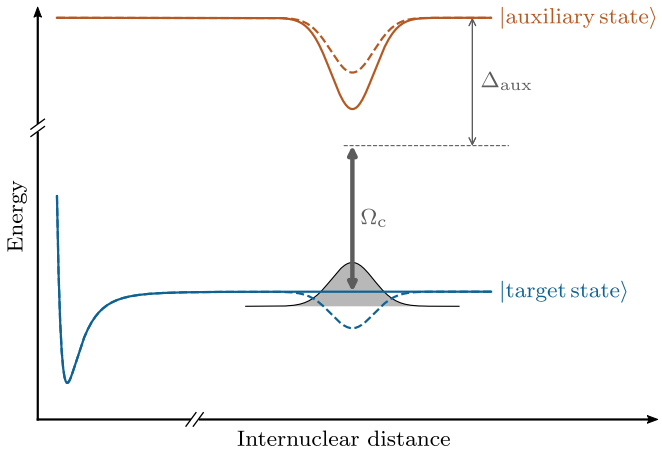

FIG. 1. Scheme for molecular potential engineering. The potential of a molecular target state (solid blue line) is strongly coupled to an excited molecular potential energy curve (solid red line), denoted as the auxiliary state. The off-resonant strong coupling Ω_c (gray arrow) with detuning Δ_{aux} modifies both potential curves (blue and red dashed lines). For sufficiently strong coupling, the low-lying potential acquires a potential well that supports a bound state (gray shaded area). The depth and shape of the potential well can be tuned by the coupling parameters. For simplicity, the additional atomic light shift of the involved states is neglected.

*herwig.ott@rptu.de

state bound in the short-range well exhibits a binding energy on the order of several $-h \times 10\,\mathrm{GHz}$ and a bond length of around $10a_0$.

As recently suggested by Wang and Côté [10], a scheme for potential engineering based on ultralong-range Rydberg molecules is ideally suited to create new potential wells at large interatomic distances in the range of hundreds to thousands of Bohr radii for otherwise only short-ranged potentials. We apply this generic idea to ultracold rubidium atoms and manipulate the molecular potential between an atom in the $5S$ and one in the $6P$ state (target state) by strong optical coupling to the molecular potential belonging to the $25D$ Rydberg state (auxiliary state) bound to a ground-state atom in the $5S$ state. To demonstrate the modification of the potential, we give experimental evidence for the appearance of a molecular bound state in the long-range well of the resulting potential.

By photoassociation spectroscopy, we experimentally find a change in binding energy for different coupling parameters and describe it with a theoretical model. With their theoretical bond length of $950a_0$, the investigated molecules are three orders of magnitude larger than the short-range part of the $5S$-$6P$ potential. We foresee that such uncommon molecular states and the underlying potential engineering scheme can be employed in the future to functionalize the molecular interaction between ground-state atoms in the ultracold regime.

To experimentally realize the proposed scheme, the proper choice of the auxiliary Rydberg state is important. The probability to create such a molecule depends on the distance distribution of the atoms in the underlying ultracold gas and longer bond length and thus higher principle quantum numbers are favored. A large optical coupling strength as well as the presence of a well isolated and deep potential well in the auxiliary potential, which allows for larger detunings from the atomic Rydberg state, on the other hand, favor low principle quantum numbers. Since we drive the coupling transition from the $6P_{3/2}$ state, we can couple to Rydberg D and S states from which we generally prefer D states for their higher ionization rates and stronger Rabi couplings. Compromising on these considerations, we choose the $25D_{5/2}$ state for which the relevant molecular potential is depicted in Fig. 2. It provides a double-well structure with a depth of about $-h \times 280\,\mathrm{MHz}$ at an interatomic distance of $850a_0$–$1100a_0$ having a sufficient probability to occur at the given density of the atomic gas. We specifically address its $m_J = 5/2$ Zeeman state to get a defined transition with maximum Rabi coupling from the fully stretched $6P_{3/2}$ $F = 3$, $m_F = 3$ state by a σ^+ transition with a Rabi frequency of $\Omega_c = 2\pi \times 293\,\mathrm{MHz}$ and varying detunings Δ_{aux} relative to the $25D_{5/2}$ Rydberg state.

The confining trap for the underlying sample of about 2×10^5 ^{87}Rb atoms in the $5S_{1/2}$ $F = 2$, $m_F = 2$ ground state is formed by a dedicated beam at 1064 nm and the crossed, strong coupling laser at 1030 nm. Due to its predominant $5S$-$6P$ character, we can photoassociate the new molecular state from the $5S$-$5S$ initial state by weakly probing on the $5S$-to-$6P$ transition. We therefore add a counterpropagating, weak probe beam at 420 nm with σ^+ polarization, Rabi frequency Ω_p, and the detuning δ_{targ} relative to the atomic, light-shifted $6P_{3/2}$ state. We apply 1000 probe pulses with a length of $10\,\mu\mathrm{s}$ while the coupling beam remains at a constant, high power for 300 ms. For the detection of the tailored molecules in the

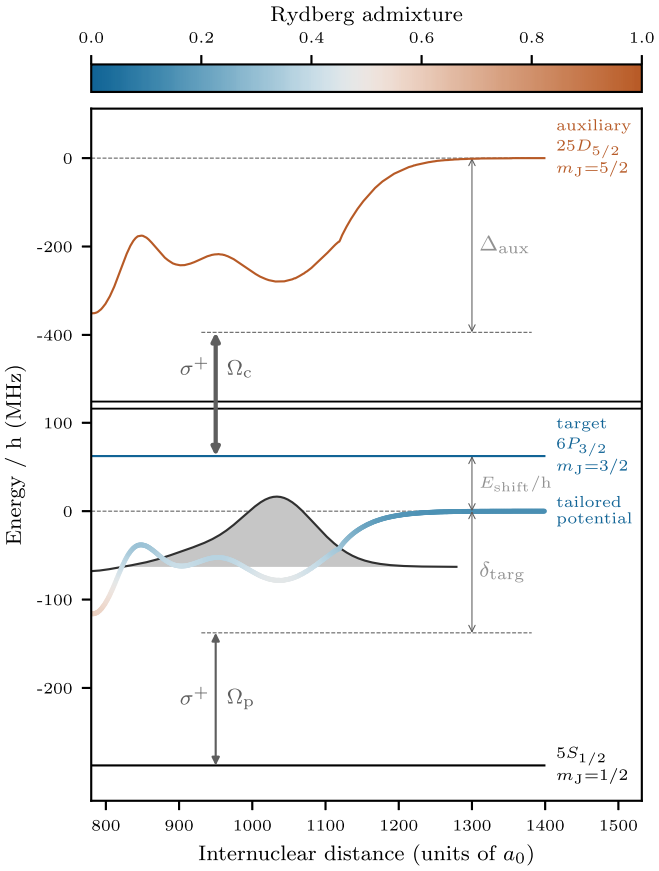

FIG. 2. Engineered molecular potential. The $6P_{3/2}$ target state with $m_J = 3/2$ (thin blue line) is strongly coupled to the $m_J = 5/2$ sublevel of the auxiliary $25D_{5/2}$ Rydberg state (thin red line) with a σ^+-polarized laser at a detuning $\Delta_{aux} = -2\pi \times 300\,\mathrm{MHz}$ and Rabi frequency $\Omega_c = 2\pi \times 293\,\mathrm{MHz}$ (gray arrow). The $5S$-$6P$ tailored potential (thick bluish line) is deformed and exhibit a modulated Rydberg state admixture (color code). In particular, the $5S$-$6P$ potential acquires a potential well, which supports a vibrational state (gray shaded area), shifted by its binding energy of $-h \times 62\,\mathrm{MHz}$. Photoassociation spectroscopy probes the $6P_{3/2}$ $m_J = 3/2$ state from the $5S_{1/2}$ $m_J = 1/2$ ground state with a weak, σ^+-polarized laser and Rabi frequency Ω_p. Since we treat the Rydberg molecule's binding mechanism separated from the coupling mechanism, we depict the system in a single-atom basis, and consider the $5S$ atom by the modulation of the Rydberg potential.

$5S$-$6P$ target potential we exploit the admixture of Rydberg character and its intrinsic ionization processes into atomic Rb^+ and molecular $Rb_2{}^+$ ions. While Rb^+ ions originate from photoionization by the dipole trap or blackbody radiation, molecular ions result from associative ionization [11]. In a small applied electric field the ions are guided to a detector and the two types of ions can be discriminated due to their different time of flight. Rydberg molecules and atomic Rydberg states differ in their dominant decay channels [12], so that we expect to find the engineered molecule's signature predominantly in one of the two signals. We therefore evaluate the two types of ions separately.

Following the probing and coupling scheme depicted in Fig. 2, we measure the spectrum shown in Fig. 3(a). The Rb^+ signal shows a strong peak around $\delta_{targ} = 2\pi \times 0\,\mathrm{MHz}$ and

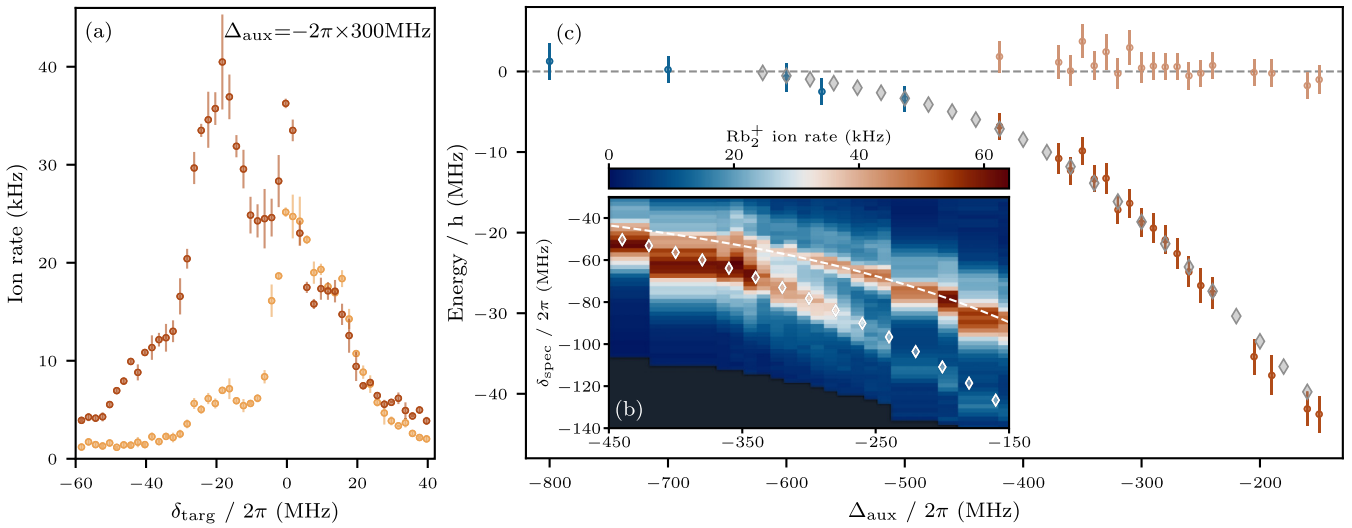

FIG. 3. Spectroscopy of the engineered $5S$-$6P$ molecules for $\Omega_c = 2\pi \times 293$ MHz. (a) Atomic Rb^+ (orange) and molecular $Rb_2{}^+$ (red) ions for the detuning of the coupling laser $\Delta_{aux} = -2\pi \times 300$ MHz. Atomic ions stem mainly from the admixture of the Rydberg state to the $6P_{3/2}$ atomic state. The peak at $\delta_{targ} = -2\pi \times 20$ MHz in the molecular ion signal indicates the presence of a bound $5S$-$6P$ state. δ_{targ} is corrected by the theoretical atomic off-resonant light shift $E_{shift} = -\hbar\Delta_{aux}/2 - \hbar\sqrt{\Omega_c^2 + \Delta_{aux}^2}/2$. The error bars denote the error of the mean. (b) We show the $Rb_2{}^+$ ion rate for different detunings Δ_{aux} of the coupling laser. The spectroscopic probing at δ_{spec} is connected to the denotations in Fig. 2 via $\delta_{spec} = \delta_{targ} + (E_{shift}/\hbar)$. The strong ion rate around the theoretical atomic off-resonant light shift (dashed line) represents the atomic state. The additionally appearing line in the map illustrates the presence of $5S$-$6P$ molecules. The binding energies are convincingly reproduced by calculated bound states in theoretically obtained potential wells that are scaled to 0.39 (white diamonds). The detuning Δ_{aux} at the right edge of the individual measurement corresponds to the experimental setting. Black regions were not measured. (c) Energies of the atomic (light red data points) and molecular states (dark red data points) in the $Rb_2{}^+$ signal for different Δ_{aux} extracted from two peak Gaussian fits. The energies are corrected by the theoretical atomic light shift. For $\Delta_{aux} < -2\pi \times 420$ MHz only a single peak can be identified (blue data points). The error bars give the error of the fitted energy and the statistical error of the light-shift correction. The theoretical energies (dashed line and diamonds) are transferred from (b).

is thus attributed to atoms in the $6P_{3/2}$ state with admixed Rydberg character. The experimental signature for the appearance of an engineered $5S$-$6P$ molecule is reflected in the $Rb_2{}^+$ signal as a strong peak at around $-2\pi \times 20$ MHz. By systematically changing the coupling between the auxiliary and the target state via the detuning of the coupling laser Δ_{aux} and recording the $Rb_2{}^+$ ion rates, we obtain the map shown in Fig. 3(b). For decreasing Δ_{aux} and thus increasing coupling strength, we find a molecular state branching from the atomic resonance. This demonstrates the continuous deformation of the target state's molecular potential and the tuning capabilities of the bound state. To extract the position of the molecular and the atomic resonance, we fit a two-peak Gaussian function to the $Rb_2{}^+$ signal. Their positions are shown in Fig. 3(c). The molecular peak is clearly separated from the atomic resonance at detunings of $\Delta_{aux} \geqslant -2\pi \times 420$ MHz and its binding energy increases to a maximum of $-h \times 40$ MHz for $\Delta_{aux} = -2\pi \times 150$ MHz.

To theoretically model our findings we consider again the scheme depicted in Fig. 2, where the difference in coupling strength for the individual Zeeman substates is neglected and a single Rabi frequency Ω_c considered, which couples the $6P_{3/2}$ $F = 3$ and the $25D_{5/2}$ state with a detuning of Δ_{aux}. Since the hyperfine interaction in the $6P_{3/2}$ state is smaller than the coupling strength Ω_c, we model the $6P_{3/2}$ state in the uncoupled fine-structure basis $|g^*\rangle := |6P_{3/2}, m_J, m_I\rangle$ and the Zeeman states of the $25D_{5/2}$ fine-structure state $|r\rangle := |25D_{5/2}, m_J, m_I\rangle$ with $I = 3/2$ for ^{87}Rb. The Hamiltonian in a single-atom basis of the form $|g^*\rangle \oplus |r\rangle$ is expressed as

$$\hat{H} = \hat{H}_0 + A_{HFS}\hat{\vec{I}} \cdot \hat{\vec{J}} + \frac{\hbar}{2}\sum_{g^*,r} \Omega_{g^*r}\, |g^*\rangle\langle r| + \text{h.c.}, \tag{1}$$

where $\hat{H}_0$ is the fine-structure Hamiltonian, A_{HFS} the hyperfine constant, and Ω_{g^*r} gives the Rabi coupling from the different $6P_{3/2}$ states $|g^*\rangle$ to the Rydberg states $|r\rangle$. The hyperfine interaction in the Rydberg state is negligible. Due to the selection rules, the Hilbert space spanned by the $|6P_{3/2}, 3/2, 3/2\rangle$ and $|25D_{5/2}, 5/2, 3/2\rangle$ state decouples for σ^+ polarization of the coupling laser and can be treated as an isolated two-level system. To ensure that we only probe this subspace in the experiment, we drive a σ^+ transition from the fully stretched $5S_{1/2}$ $F = 2$, $m_F = 2$ ground state, composed of solely the $m_J = 1/2$ component. With the spatially varying energy $V_{mol}(R)$ of the Rydberg molecular potential the system is thus described by

$$\hat{H}(R) = \hbar\begin{pmatrix} 0 & \Omega_c/2 \\ \Omega_c/2 & \Delta_{aux} + V_{mol}(R)/\hbar \end{pmatrix}. \tag{2}$$

Figure 2 shows the lower eigenvalues along with the target and auxiliary states of the system as a function of R for typical experimental parameters. The resulting potential is a mixture of both states and comprises the engineered potential we are aiming for. At large R the energy difference between the diagonalization result and the target state is given by the

ac Stark shift $E_{\text{shift}} = -\hbar\Delta_{\text{aux}}/2 - \hbar\sqrt{\Omega_c^2 + \Delta_{\text{aux}}^2}/2$. From the eigenvectors of Eq. (2) we extract the local Rydberg state admixture and depict it color coded in Fig. 2. Via a shooting method we determine the vibrational bound states in the resulting $5S$-$6P$ potential and identify the lowest bound state that localizes mostly in the outer double well. By weighting the local Rydberg admixtures with the vibrational wave function, we find an overall Rydberg admixture of about 43% for the designed molecule in Fig. 3(a).

The extracted binding energies of the bound states are shown in Fig. 3(c) as gray diamonds. To match the experimentally measured spectra, the calculated molecular potential has been scaled by a factor of 0.39 prior to the calculation of the bound states. The reason for this mismatch might stem from neglecting the state mixing in the Rydberg state due to the Rydberg molecular interaction, which will lead to less $m_J = 5/2$ character in the auxiliary state and consequently to an R-dependent, generally lower Rabi frequency. Apart from this scaling factor, the agreement with the measured spectra is good and the trend of the experimental data as well as the detaching point from the atomic resonance are well reproduced. The spectroscopic result along with the simple two-level model demonstrate the ability to deform a target potential to engineer molecular long-range potentials supporting bound states.

While the short lifetime of the $6P$ state might limit the applications of our specific realization in ultracold gases, it is important to note that the demonstrated mechanism is generic for all atom pairs, which can be coupled to a Rydberg molecule. This includes in particular two ground-state atoms, which are coupled with a single photon transition to a Rydberg molecular potential. Because the ground-state molecules are stable, only the admixture of the Rydberg molecules shortens the lifetime. As a consequence, much lower Rabi frequencies are required to create a bound state between the two ground-state atoms. Realistic estimates for the Rabi frequency of $2\pi \times 5\,\text{MHz}$ and detuning of $-2\pi \times 2\,\text{MHz}$ suggest a binding energy of about $-h \times 25\,\text{kHz}$ at a molecular lifetime of more than 5 ms. Such conditions would open up plenty of opportunities for ultracold molecular physics. As the binding energy of the engineered molecules is tunable up to the limit of two free atoms, the creation of halo states [13], which have a large part of their wave function in the classically forbidden region and thus have an enormous spatial extent, is possible. Furthermore, the inherent tuning capabilities allow to continuously move the bound state into the continuum. When the bound state crosses the threshold, the conditions to observe Efimov physics [14] are given. In previous studies on ultracold atomic gases [15], the tuning of the two-body bound states was done with the help of a Feshbach resonance. Thereby, loss into deeply bound molecular states is unavoidable. In our approach, there are no deeply bound molecular states, as the relevant part of the two-body molecular potential has its well outside the short-range part of the normal pair potential. Our technique might therefore allow the observation of three-body bound states under clear conditions with low intrinsic losses. Lastly, different realizations of optical Feshbach resonances [2] are feasible with our approach.

The data that support the plots within this Letter and other findings of this study are available from the corresponding author upon request.

We would like to thank R. Côté for helpful discussions. We acknowledges financial support by the DFG within Project OT 222/8-1 and the collaborative research center TR185 OSCAR, Project B2 (No. 277625399). This work was also supported by the Max Planck Graduate Center with the Johannes Gutenberg-Universität Mainz (MPGC).

T.K., P.M., and J.B. performed the experiments. T.K. and P.M. analyzed the data. T.K. performed the molecular potential calculations and prepared the initial version of the manuscript. H.O. conceived the project. H.O. and T.N. supervised the experiment. All authors contributed to the data interpretation and manuscript preparation.

The authors declare no competing financial interests.

[1] C. Chin, R. Grimm, P. Julienne, and E. Tiesinga, Feshbach resonances in ultracold gases, Rev. Mod. Phys. **82**, 1225 (2010).

[2] O. Thomas, C. Lippe, T. Eichert, and H. Ott, Experimental realization of a Rydberg optical Feshbach resonance in a quantum many-body system, Nat. Commun. **9**, 2238 (2018).

[3] C. A. Regal, C. Ticknor, J. L. Bohn, and D. S. Jin, Creation of ultracold molecules from a Fermi gas of atoms, Nature (London) **424**, 47 (2003).

[4] E. A. Donley, N. R. Claussen, S. T. Thompson, and C. E. Wieman, Atom-molecule coherence in a Bose-Einstein condensate, Nature (London) **417**, 529 (2002).

[5] M. Greiner, C. A. Regal, and D. S. Jin, Emergence of a molecular Bose-Einstein condensate from a Fermi gas, Nature (London) **426**, 537 (2003).

[6] S. Jochim, M. Bartenstein, A. Altmeyer, G. Hendl, S. Riedl, C. Chin, J. Hecker Denschlag, and R. Grimm, Bose-Einstein condensation of molecules, Science **302**, 2101 (2003).

[7] J. L. Bohn, A. M. Rey, and J. Ye, Cold molecules: Progress in quantum engineering of chemistry and quantum matter, Science **357**, 1002 (2017).

[8] S. Hollerith, K. Srakaew, D. Wei, A. Rubio-Abadal, D. Adler, P. Weckesser, A. Kruckenhauser, V. Walther, R. van Bijnen, J. Rui, C. Gross, I. Bloch, and J. Zeiher, Realizing Distance-Selective Interactions in a Rydberg-Dressed Atom Array, Phys. Rev. Lett. **128**, 113602 (2022).

[9] Y. Liu and K.-K. Ni, Bimolecular chemistry in the ultracold regime, Annu. Rev. Phys. Chem. **73**, 73 (2022).

[10] J. Wang and R. Côté, Ultralong-range molecule engineering via Rydberg dressing, Phys. Rev. Res. **2**, 023019 (2020).

[11] T. Niederprüm, O. Thomas, T. Manthey, T. M. Weber, and H. Ott, Giant Cross Section for Molecular Ion Formation in Ultracold Rydberg Gases, Phys. Rev. Lett. **115**, 013003 (2015).

[12] M. Schlagmüller, T. C. Liebisch, F. Engel, K. S. Kleinbach, F. Böttcher, U. Hermann, K. M. Westphal, A. Gaj, R. Löw, S. Hofferberth, T. Pfau, J. Pérez-Ríos, and C. H. Greene, Ultracold Chemical Reactions of a Single Rydberg Atom in a Dense Gas, Phys. Rev. X **6**, 031020 (2016).

[13] S. Zeller, M. Kunitski, J. Voigtsberger, A. Kalinin, A. Schottelius, C. Schober, M. Waitz, H. Sann, A. Hartung, T. Bauer, M. Pitzer, F. Trinter, C. Goihl, C. Janke, M. Richter,

G. Kastirke, M. Weller, A. Czasch, M. Kitzler, M. Braune *et al.*, Imaging the He_2 quantum halo state using a free electron laser, Proc. Natl. Acad. Sci. USA **113**, 14651 (2016).

[14] P. Naidon and S. Endo, Efimov physics: A review, Rep. Prog. Phys. **80**, 056001 (2017).

[15] T. Kraemer, M. Mark, P. Waldburger, J. G. Danzl, C. Chin, B. Engeser, A. D. Lange, K. Pilch, A. Jaakkola, H.-C. Nägerl, and R. Grimm, Evidence for Efimov quantum states in an ultracold gas of caesium atoms, Nature (London) **440**, 315 (2006).